

Acknowledgment. I am grateful to Dr. R. Klimes (Korean Sahmyook Univ.) for his critical comments on correct English writing and, to Dr. J. R. OH (Chemical Oceanography Lab. of *Korea Ocean Research & Development Institute*) for his assist in seawater sampling.

References

1. P. F. Siligman, J. G. Grovhoug, A. O. Valkirs, P. M. Stang, R. Fransham, M. O. Stallard, B. Davidson, and R. F. Lee, *Appl. Organomet. Chem.*, **3**, 31 (1989).
2. S. J. Blunder and Chapman, Organotin compounds in the environment. In: *Organometallic compounds in the environment*, P. J. Craig, ed Longman, London, p. 111 (1986).
3. C. Alzieu, TBT determinantal effects on oyster culture in France evolutionsince antifouling paint regulation. In: *Proc. Organotin. Symposium, Oceans-86 Conference, Washington, DC, IEEE, New York*, **4**, 1130 (1986).
4. D. Chagot, C. Alzieu, J. Sanjuan, and H. Grizel, *Aquat. Living Resource*, **3**, 121 (1990).
5. C. Alzieu, *et al.*, *Rev. Trav. Inst. Peches Marit.*, **44**, 301 (1980).
6. G. W. Bryan, P. E. Gibbs, Hummerstone, and G. R. Gand Burt, *J. Mar. Biol. Ass. UK*, **66**, 611 (1986).
7. D. Chagot, C. Alzieu, J. Sanjuan, and H. Crizel, *Aquat Living Resour.*, **3**, 121 (1990).
8. S. J. Blunden and A. Chapman, Ref. 1, p. 138.
9. O. X. F. Donald, Tin and germanium. In: *Environmental Analysis using Chromatography Interfaced with Atomic Spectroscopy*, R. M. Harrison, and S. Rapsomanikiss (eds), Ellis Horwood, 194 (1989).
10. J. A. Jackson, W. R. Blair, F. E. Brinckman, and W. P. Iverson, *Environ. Sci. Technol.*, **16**, 110 (1982).
11. M. D. Müller, *Anal. Chem.*, **59**, 617 (1987).
12. K. Sasaki, T. Ishizaka, T. Suzuki, and Y. Saito, *J. Assoc. Off. Anal. Chem.*, **71**(2), 360 (1988).
13. J. L. Gomez-Ariza, E. Morales, and M. Ruiz-Benites, *Appl. Organomet. Che.*, **6**, 279 (1992).
14. K. Takahashi, *J. Japanese Chem. Soc.*, **5**, 367 (1991).
15. P. Michel and B. Averty, *Appl. Organomet. Chem.*, **5**, 393 (1991).

A Green's-Matrix Approach to Chemisorption

Yun Hee Jang and Hojing Kim*

Department of Chemistry, Seoul National University, Seoul 151-742

Research Institute of Molecular Sciences, Seoul National University, Seoul 151-742

Received October 9, 1992

A self-consistent-field Green's matrix method for the calculation of electronic properties of chemisorbed system is devised and applied to the methanol on copper(110) surface. The method is based on CNDO Hartree-Fock approximation. Contour integration in the complex energy plane is used for an efficient calculation of the charge-density bond-order matrix. The information on each fragment prior to chemisorption is efficiently used and a small number of iterations are needed to reach the self-consistency. The changes of density of states and other quantities of methanol due to chemisorption are consistent with reported experimental results.

Introduction

Electronic processes in chemisorption and catalytic action of metal surfaces play fundamental roles in chemistry and chemical industry. Until now, two calculational methods have commonly been used to address problems of this nature: cluster method and slab method. Cluster method models a surface as a group of a few atoms. This permits direct use of highly developed computer programs of quantum chemistry. Since chemisorption is known to be a local phenomenon and an adsorbate is coupled to only a few atoms near the chemisorption site,^{1,2} this approach to chemisorption is reasonable. However, the convergence of the results with cluster size is left open to question.^{3,4} Slab method(band calculation) simulates the solid with a finite number of layers having two-dimensional periodicity. This method takes a surface as infinite periodic repetitions of a unit cell. However, since the perturbation due to chemisorption breaks the translat-

ional symmetry of the surface and the complexity grows rapidly with the number of atoms in the unit cell, the slab calculation for chemisorbed system is a complicated problem requiring larger unit cell, especially in a low coverage.^{3,5,6}

The Green's function, which has been used in mathematics and physics to solve an inhomogeneous differential equation in terms of the solution of corresponding homogeneous equation,⁷ permits the study of a complicated perturbed system by representing it as a relatively simple unperturbed system plus a small perturbation.⁸ The Green's-function approach to a local perturbation in a periodic system was originated by Koster and Slater and by Anderson,^{9,10} and it was further developed by Callaway and Hughes.¹¹ An LCAO matrix form of this method was investigated by Pantelides.^{12,13} The self-consistent field treatment was given by Feibelman in density-functional formalism¹⁴ and by Ladik and Seel in Hartree-Fock scheme.^{14,15}

We apply the self-consistent field Green's-function app-

roach to chemisorption on transition metal surface. A combined system of the unperturbed surface and free adsorbate molecule is subjected to the perturbation due to chemisorption. It exploits the short range of the perturbation due to chemisorption. The information of each fragment prior to chemisorption is efficiently utilized to obtain the electronic structure of chemisorbed system. We use this feature to obtain the self-consistent electronic structure of chemisorbed system more easily and to reproduce the experimentally obtained UPS spectrum of chemisorbed system.

The CNDO Hartree-Fock approximation is used in this approach, because it is appropriate to study a reasonable size of transition metal clusters representing the chemisorption site.¹⁶⁻²¹

Theory

We try to solve the Hartree-Fock-Roothaan equation for chemisorbed system in CNDO approximation

$$(E\mathbf{1} - \mathbf{F})\mathbf{C} = \mathbf{0}, \quad (1)$$

where \mathbf{F} is Fock matrix and \mathbf{C} stands for wavefunction coefficients.²² $\mathbf{1}$ is a unit matrix. Fock matrix is given by

$$F_{\mu\mu} = h_{\mu\mu} - \frac{1}{2} P_{\mu\mu} \gamma_{\mu\mu} + \sum_{\lambda} P_{\lambda\lambda} \gamma_{\mu\lambda}, \quad (2)$$

$$F_{\mu\nu} = h_{\mu\nu} - \frac{1}{2} P_{\mu\nu} \gamma_{\mu\nu}, \quad (3)$$

where P is a charge-density bond-order matrix and $h_{\mu\nu}$ defines the element of the core hamiltonian matrix h .^{23,24} $\gamma_{\mu\nu}$ and $\gamma_{\nu\mu}$ represent the one- and two-center two-electron integrals. The electronic energy is given by

$$E_{elec} = \frac{1}{2} \sum_{\mu} \sum_{\nu} P_{\mu\nu} (h_{\mu\nu} + F_{\nu\mu}). \quad (4)$$

The unperturbed system is defined as adsorbate plus substrate without interaction. This system is represented by the solution of

$$(E\mathbf{1} - \mathbf{F}^0)\mathbf{C} = \mathbf{0}, \quad (5)$$

where

$$\mathbf{F}^0 = \begin{pmatrix} \mathbf{F}_{ads}^0 & \mathbf{0} \\ \mathbf{0} & \mathbf{F}_{subs}^0 \end{pmatrix}. \quad (6)$$

\mathbf{F}_{ads}^0 and \mathbf{F}_{subs}^0 are the self-consistent Fock matrices of free adsorbate and unperturbed substrate metal, respectively. \mathbf{F}_{subs}^0 is of infinite or large dimension.

The Green's matrix $\mathbf{G}^0(E)$ of unperturbed system of defined by^{3,8-15}

$$(E\mathbf{1} - \mathbf{F}^0)\mathbf{G}^0(E) = \mathbf{1} \quad (7)$$

and is calculated by matrix inversion

$$\mathbf{G}^0(E) = (E\mathbf{1} - \mathbf{F}^0)^{-1} = \begin{pmatrix} \mathbf{G}_{ads}^0 & \mathbf{0} \\ \mathbf{0} & \mathbf{G}_{subs}^0 \end{pmatrix}, \quad (8)$$

where

$$\mathbf{G}_{ads}^0(E) = (E\mathbf{1} - \mathbf{F}_{ads}^0)^{-1}, \quad (9)$$

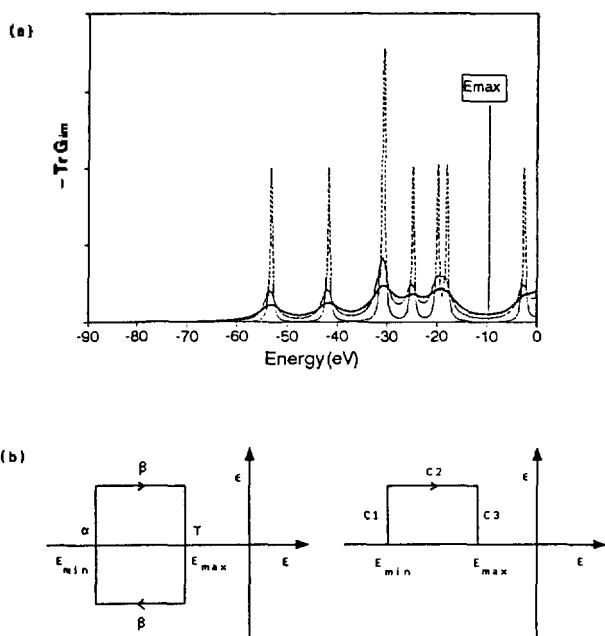


Figure 1. (a) The negative trace of the imaginary Green's matrix evaluated along paths parallel to the real axis. The distance ϵ from real axis is varied. Dashed, solid and heavy solid curves are for $\epsilon = 2.72$, 1.36 and 0.27 eV, respectively. Note that it has very sharp structures near the real axis (small ϵ), while it is well-behaved, smooth, and easy to integrate in the complex plane (large ϵ). (b) The energy-integration contour in obtaining the charge-density bond-order matrix from Green's matrix. It has been displaced from real axis into the complex plane. The contour can be reduced to the upper half.

$$\mathbf{G}_{subs}^0(E) = (E\mathbf{1} - \mathbf{F}_{subs}^0)^{-1}. \quad (10)$$

Perturbation consists of turning on the interaction between adsorbate and substrate. The exact form of the perturbation \mathbf{V} due to chemisorption is not known. We define the perturbation \mathbf{V} as the deviation of Fock matrix of chemisorbed system from that of unperturbed system,^{3,8,15}

$$\mathbf{V}(E) = \mathbf{F} - \mathbf{F}^0 = (E\mathbf{1} - \mathbf{F}^0) - (E\mathbf{1} - \mathbf{F}). \quad (11)$$

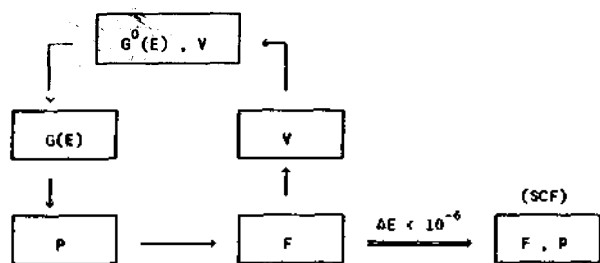
Then the Dyson equation

$$\mathbf{G}(E) = \mathbf{G}^0(E) + \mathbf{G}^0(E) \mathbf{V}(E) \mathbf{G}(E), \quad (12)$$

or

$$\mathbf{G} = (\mathbf{1} - \mathbf{G}^0 \mathbf{V})^{-1} \mathbf{G}^0 \quad (13)$$

is derived. Since we don't have an exact Fock matrix \mathbf{F} for chemisorbed system, we have to perform an SCF iteration, beginning with an initial guess of \mathbf{F} and \mathbf{V} . We take an initial guess of \mathbf{V} , considering only the "static" perturbation prior to the charge redistribution of one fragment (adsorbate or substrate) due to the other fragment.²⁵ Beginning with $\mathbf{G}^0(E)$ of the unperturbed system and $\mathbf{V}(E)$, a new Green's matrix $\mathbf{G}(E)$ is obtained by the Dyson equation. Since the perturbation due to chemisorption affects only a few atoms near the chemisorption site,^{1,2} only a finite number of the elements of \mathbf{V} will be different from zero and, approximately, the size of Dyson equation is determined by the range of \mathbf{V} and the equation can be solved as a finite matrix equation.³ This



Scheme 1. Iteration scheme in self-consistent field Green's matrix method.

is the same concept as that of the cluster model.

The charge-density bond-order matrix P can be computed by integration of $G(E)dE$ up to the Fermi energy.^{8,14}

$$P_{\mu\nu} = 2 \frac{1}{2\pi i} \int_C dE G_{\mu\nu}(E) \quad (14)$$

where the integral path C includes all the occupied states. This integration has been conventionally performed along the real energy axis.¹⁴ However, along the real energy axis, the Green's matrix elements mostly vary rapidly with energy due to the poles, so that an accurate evaluation of the integral requires a knowledge of G on a very fine mesh of E values (dashed line in Figure 1(a)). The integration can be carried out more efficiently by displacing the integration path C from the real energy axis to a contour in the complex energy plane (See Figure 1(b)).^{8,26,27} Since the imaginary part of G is smooth function of energy along this path, a small number of sampling points are sufficient to compute the charge-density bond-order matrix P (solid line in Figure 1(a)). Detailed expressions will be presented in Appendix.

A new Fock matrix F is obtained from P , and the electronic energy is calculated from F and P . A new Green's matrix $G(E)$ is calculated from new F , and so on. This procedure is carried out repeatedly until the difference in the electronic energies from two consecutive iterations is below a certain threshold.^{13,14} The self-consistent Green's matrix approach can be summarized as follows (See Scheme 1):

- (1) Calculate $G^0(E)$, the Green's matrix of the unperturbed system.
- (2) Calculate a first guess for $V(E)$.
- (3) Solve the Dyson equation, for a number of E points, to get a new Green's matrix $G(E)$.
- (4) Calculate a new charge-density bond-order matrix P from $G(E)$.
- (5) Calculate a new F from P .
- (6) Calculate a new $V(E)$.
- (7) The steps are repeated from step (2) on, until the self-consistency is reached

Having reached the self-consistency, the eigenvalues and wavefunctions are obtained by diagonalizing the self-consistent Fock matrix F . We calculate the various quantities from these.²⁸

Computations

We present the results of a calculation in which the above formalism is applied. We study the adsorption of methanol on copper(110) surface. Copper is known as a selective oxi-

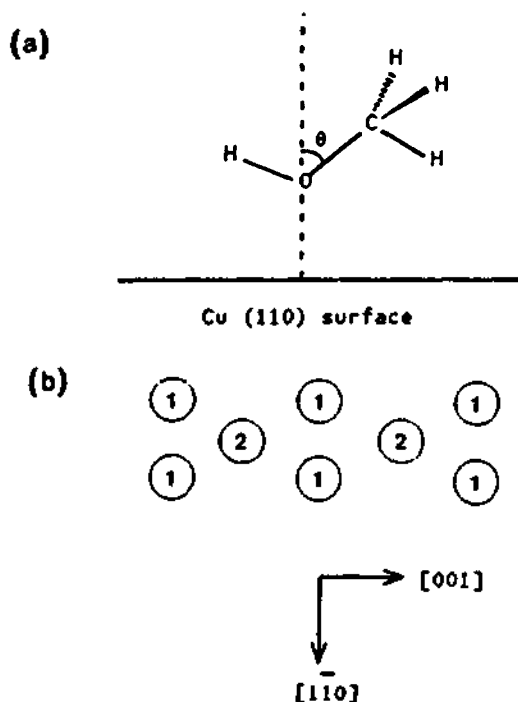


Figure 2. (a) Structural model for methanol on Cu(110). We have assumed $\theta = 36^\circ$ in $[001]$ direction. (b) $\text{Cu}_6(6,2)$ cluster as a model of 2-fold bridge site of Cu(110) surface. 1 and 2 represent for the first and second layer atoms, respectively.

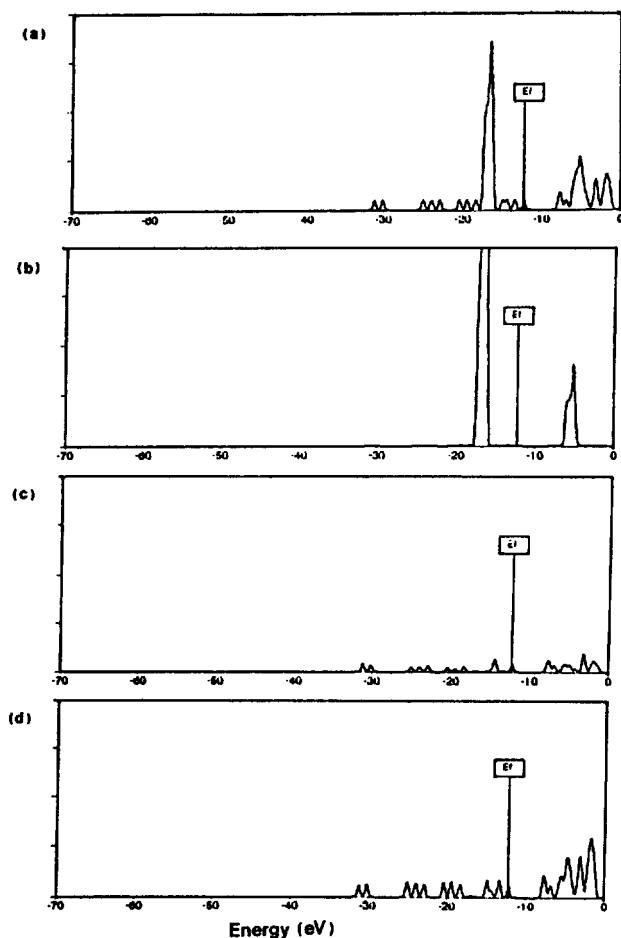
dation catalyst in the conversion of methanol to aldehyde.²⁹⁻³¹ It has the ability to remove hydrogen atom from the alcohol without breaking the C-O bond.^{29,30} However, bulk copper is not active toward the decomposition of methanol and oxygen must be present in the copper for it to be active.^{29,31} It is interesting to consider the interaction of methanol and copper surface with and without oxygen. As the first step, we study the interaction between methanol and copper surface without preadsorbed oxygen.

Although we study methanol on copper(110) surface only, this work can be generalized to represent the interaction between methanol and various copper surfaces. Sexton showed that very little difference existed between the experimental results for methanol/Cu(110) and methanol/Cu(100).³⁰

The adsorption site and geometry of methanol on copper (110) surface is fixed as obtained from experiments for methanol or methoxide adsorbed on copper or other metal surfaces. The adsorption site has been determined to be a mixture of two-fold bridge site and four-fold hollow site.³²⁻³⁵ We assume that methanol is chemisorbed at the two-fold short-bridge site. The tilt angle of C-O axis from surface normal is fixed as 36° in $[001]$ direction from the results of Holup-Krappner, of Bader and of Outka (See Figure 2).³²⁻³⁴ The Cu-O bond length is fixed as 1.97 \AA , which is obtained by Linder and for copper-methoxy coordination compounds.³⁵⁻³⁷ The C-O bond distance is fixed as 1.41 \AA of copper-methanol and copper-methoxy compounds.³⁷⁻³⁹ The O-H bond length and C-O-H bond angle are assumed to be 1.0 \AA and 109.5° , respectively.⁴⁰ To represent the two-fold short-bridge site of Cu(110) surface, $\text{Cu}_6(6,2)$ cluster is used (See Figure 2). Cu-Cu nearest neighbor distance is fixed to 2.56 \AA of bulk cop-

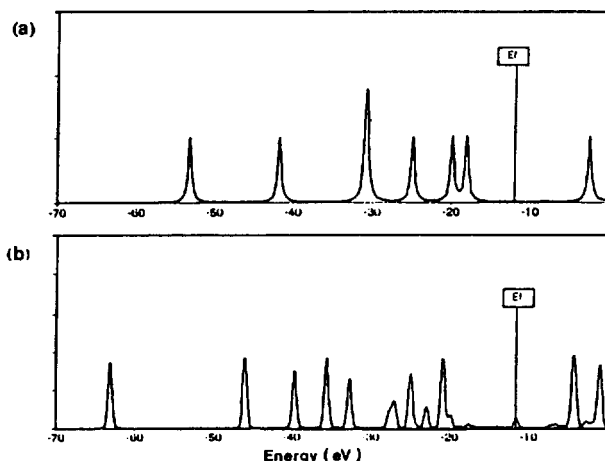
Table 1. CNDO/2 Parameters for Copper (in eV)

	Core integral	Bonding parameter	Slater exponent
Cu 4s	4.567	7.726	1.950
Cu 4p	1.347	7.726	1.200
Cu 3d	6.520	20.292	3.733
H 1s	13.476	9.000	1.300
C 2s	20.351	21.000	1.500
C 2p	11.872	21.000	1.325
O 2s	31.690	31.000	2.200
O 2p	15.411	31.000	1.975

**Figure 3.** Total and projected DOS of Cu₈ cluster. (a) total DOS. (b)-(d) projected DOS of 3d, 4s(×5) and 4p(×5). E_f indicates the HOMO energy level of the Cu₈ cluster.per.³⁴

The CNDO parameters are taken from the work of Böhm and Gleiter and listed in Table 1.²¹ The values of β^0 for copper are chosen to be nearly equal to the negatives of the first and second ionization potentials.⁴⁴⁻⁴³ We calculate the density of states(DOS) of Cu₈ cluster to see the validity of these parameter and show these in Figure 3. The projected densities of states(PDOS's) of 3d, 4s and 4p orbitals are shown together. DOS and PDOS are calculated by^{44,45}.

$$\rho_{\nu}(E) = -\frac{1}{\pi} \text{Im} G_{\nu\nu}(E), \quad (15)$$

**Figure 4.** (a) DOS of free methanol. E_f indicates the HOMO level of Cu₈ cluster. (b) PDOS(×2.5) of methanol chemisorbed on Cu₈ cluster. E_f indicates the HOMO energy level of chemisorbed system.**Table 2.** Number of Valence Electrons of Free Methanol Evaluated Along Various Integration Paths. Distance of *c*2 in Figure 1 from Real Axis(ϵ) is Varied. The Average Spacing Between Mesh Points Along *c*2 are Varied. The Spacing Along *c*1 and *c*3 are Fixed. The Upper and Lower Limit are Fixed. A Small Number of Mesh Points are Sufficient to Give Converged Result when ϵ is 1.36 eV

Average spacing	Number of mesh points	Number of valence electrons	
		($\epsilon=1.36$ eV)	($\epsilon=0.27$ eV)
0.93	80	12.40	7.45
0.74	100	13.94	12.13
0.57	130	13.97	13.62
0.41	185	13.98	13.60
0.27	270	13.98	13.61
0.09	780		13.95

$$\rho(E) = -\frac{1}{\pi} \sum_{\mu} \{ \text{Im} G_{\mu\mu}(E) \} = -\frac{1}{\pi} \text{Tr} \{ \text{Im} G(E) \}. \quad (16)$$

The highest occupied molecular orbital(HOMO) is positioned at about -12 eV, while the Fermi level of bulk copper is known to be about -5 eV.⁴⁶⁻⁴⁸ However, the relative position of peaks is more important. The 3d band position is about 5 eV below the HOMO level. Near the HOMO level the 4s and 4p orbitals have main contributions. These agree with the experimental or other calculational results.^{46,47}

It is known from experiments that HOMO of methanol is at about 5.8 eV below the Fermi level of copper.^{48,49} We shift the entire energy levels of methanol to reproduce these experimental results. DOS of free methanol is shown in Figure 4(a).

Results and Discussion

First, we perform the CNDO calculation for each of the unperturbed system (free methanol and Cu₈ cluster) to give

Table 3. Wiberg Indices for Methanol Before and after Chemisorption

	Before chemisorption	After chemisorption	Change during chemisorption
C-O	1.099* (1.049)**	0.920	-0.179 (-0.124)
O-H	0.934 (0.870)	0.840	-0.094 (-0.030)

*for free methanol. **for isolated methanol with its geometry fixed as given from the experimental results for methanol adsorbed on metal surfaces

F_{ad}^0 and F_{sub}^0 . Then, we perform the iterative calculation to obtain the self-consistent Green's matrix of chemisorbed system (methanol adsorbed on Cu_8 cluster). We perform the contour integration along the rectangular integration path shown in Figure 1(b). We use the trapezoidal rule in numerically evaluating the integral.^{6,50} In order to determine the optimum path of integration, we calculate the number of valence electrons of free methanol from the charge-density bond-order matrix obtained along various integration paths (See Table 2). When the distance ϵ of parallel part of contour from the real axis is 1.36 eV, the results show the converged behaviour for average spacings less than 0.57 eV, and we take these values. The points are not chosen equidistantly, so that the mesh is denser near HOMO. The requirement on the chosen contour is that it encloses all occupied states. Since the sharp structures of $G(E)$ on the real axis are broadened in complex energy plane, they lose the physical meaning as state-densities.^{7,30} Thus we must be careful to determine upper and lower integration limit (E_{max} and E_{min} in Figure 1(b)). We take about -80 eV and about -9 eV as lower and upper limit, respectively, because the structures in Figure 1(a) approach zero near these energy points and the reasonable number of valence electrons for each system is obtained when we integrate between these limits.

After about 40 iterations, the energy difference of 2.2×10^{-5} eV is obtained between two consecutive iterations, which is below our threshold for self-consistency (3.0×10^{-5} eV). A smaller number of iterations are needed to reach the self-consistency, compared to the conventional SCF calculation. This is because our calculation starts from the converged data of two fragments. The knowledge of each fragment is efficiently utilized to obtain the electronic structure of combined system.

We show PDOS of methanol chemisorbed on Cu_8 cluster in Figure 4(b) with the HOMO level of chemisorbed system. The shape and the relative position of peaks near HOMO are almost the same as those of UPS spectra obtained by Sexton and Hughes.⁴⁹ We have adjusted the CNDO parameters to reproduce the experimentally determined differences of the energy levels of adsorbate from those of substrate. Since the self-consistency is easily obtained with these adjusted parameters in our approach, this approach can be used to predict the UPS spectrum of the chemisorbed system.

We calculate wiberg indices for C-O and C-H bonds of methanol and they are given in Table 1. The wiberg bond order index is defined by^{51,52}

$$B_{AB} = \sum_{i \in A} \sum_{j \in B} P_{ij}^2, \quad (17)$$

where A and B indicate the atoms of interest. This is a measure of overlap electron density between two atoms and can be used to characterize changes in chemical bonding. The wiberg index of O-H bond is hardly decreased during chemisorption compared to that of C-O bond. This is consistent with the fact that copper is not active to the oxidation of methanol to formaldehyde in the absence of preadsorbed oxygen.^{30,31}

Conclusion

A self-consistent-field Green's-matrix method for the calculation of electronic properties of chemisorbed system is described in detail and applied to the methanol/ $Cu_8(110)$ cluster. The method is based on CNDO Hartree-Fock approximation and the cluster model is used to simulate the metal surface. We use the contour integration in the complex energy plane for an efficient calculation of charge-density bond-order matrix. The information on each fragment prior to chemisorption is efficiently used and a small number of iterations are need to reach the self-consistency. We obtain the density of states(DOS) of methanol before and after chemisorption. The relative positions and shapes of peaks near HOMO are almost the same as those of UPS spectra. The wiberg index of O-H bond is hardly decreased during chemisorption compared to that of C-O bond. This is consistent with the experimental results that copper, without preadsorbed oxygen, have small catalytic activity to oxidation of methanol.

Acknowledgement. This work is supported by Korea Science and Engineering Foundation, S.N.U. Daewoo Research Fund and Ministry of Education.

References

1. K. Hermann, P. S. Bagus, and C. J. Nelin, *Phys. Rev. B*, **35**, 9467 (1987).
2. S. Hwang, Y. H. Jang, and H. Kim, *Bull. Korean Chem. Soc.*, **12**, 635 (1991).
3. P. J. Feibelman, *Phys. Rev. Lett.*, **54**, 2627 (1985).
4. D. Post and E. J. Baerends, *Chem. Phys. Lett.*, **86**, 176 (1982).
5. Y. B. Band and S. Efrima, *Phys. Rev. B*, **28**, 4126 (1983).
6. P. J. Feibelman, *Phys. Rev. B*, **35**, 2626 (1987).
7. P. M. Morse and H. Feshbach, *Methods of Theoretical Physics*, McGraw-Hill (1953).
8. A. R. Williams, P. J. Feibelman, and N. D. Lang, *Phys. Rev. B*, **26**, 5433 (1982).
9. G. F. Koster and J. C. Slater, *Phys. Rev.*, **95**, 1167 (1954).
10. P. W. Anderson, *Phys. Rev.*, **124**, 41 (1961).
11. J. Callaway and A. J. Hughes, *Phys. Rev.*, **156**, 860 (1967).
12. J. Bernholc and S. T. Pantelides, *Phys. Rev. B*, **18**, 1780 (1978).
13. J. Pollman and S. T. Pantelides, *Phys. Rev. B*, **18**, 5524 (1978).
14. M. Seel, *Int. J. Quant. Chem.*, **26**, 753 (1984).
15. O. Fleck and J. Ladik, *Int. J. Quant. Chem.*, **39**, 839 (1991).
16. J. A. Pople, D. P. Santry and G. A. Segal, *J. Chem. Phys.*, **43**, S129 (1965).
17. J. A. Pople and G. A. Segal, *J. Chem. Phys.*, **43**, S136 (1965).

18. J. A. Pople and G. A. Segal, *J. Chem. Phys.*, **44**, 3289 (1966).
19. D. W. Clack, N. S. Hush, and J. R. Yandle, *J. Chem. Phys.*, **57**, 3503 (1972).
20. G. Blyholder, *J. Chem. Phys.*, **62**, 3193 (1975).
21. M. C. Böhm and R. Gleiter, *Theoret. Chim. Acta*, **59**, 127 (1981).
22. C. C. J. Roothaan, *Rev. Mod. Phys.*, **23**, 69 (1951).
23. J. A. Pople and D. L. Beveridge, *Approximate Molecular Orbital Theory*, McGraw-Hill (1970).
24. J. Sadlej and I. L. Cooper, *Semi-empirical Methods of Quantum Chemistry*, Ellis Horwood Limited (1985).
25. A. J. Grand and B. T. Pickup, *Int. J. Quant. Chem.*, **40**, 97 (1991).
26. P. Krüger and J. Pollman, *Phys. Rev. B*, **38**, 10578 (1988).
27. R. Zeller, J. Deutz, and P. H. Dederichs, *Solid State Commun.*, **44**, 993 (1982).
28. A. Szabo and N. S. Ostlund, *Modern Quantum Chemistry*, Macmillan Pub. (1982).
29. M. A. Chesters and E. M. McCash, *Spectrochim. Acta*, **43A**, 1625 (1987).
30. B. A. Sexton, *Surface Sci.*, **88**, 299 (1979).
31. I. E. Wachs and R. J. Madix, *J. Catal.*, **53**, 208 (1978).
32. E. Holub-Krappe, *et al.*, *Surface Sci.*, **173**, 176 (1986).
33. M. Bader, A. Puschmann, and J. Haase, *Phys. Rev. B*, **33**, 7336 (1986).
34. D. A. Outka, R. J. Madix, and J. Stöhr, *Surface Sci.*, **164**, 235 (1985).
35. Th. Linder, *et al.*, *Surface Sci.*, **203**, 333 (1988).
36. C. Fukuhara, *et al.*, *Bull. Chem. Soc. Jpn.*, **62**, 3939 (1989).
37. R. D. Willett and G. L. Breneman, *Inorg. Chem.*, **22**, 326 (1983).
38. S. K. Mandal, *et al.*, *Can. J. Chem.*, **65**, 2815 (1987).
39. D. R. Yarkony, *et al.*, *J. Am. Chem. Soc.*, **96**, 656 (1974).
40. S. M. Gates, *et al.*, *Surface Sci.*, **146**, 199 (1984).
41. O. V. Sizova, *et al.*, *Zh. Strukt. Khim.*, **24**, 125 (1983).
42. A. N. Ermoshkin, *et al.*, *Phys. Stat. Sol.*, **118**, 191 (1983).
43. B. E. Douglas, *Inorganic Chemistry*, 2nd ed. (1983).
44. E. N. Economou, *Green's Functions in Quantum Physics*, Springer-Verlag (1979).
45. S. K. Lyo and R. Gomer, *Interactions on Metal Surfaces*, ed. by R. Gomer, Springer-Verlag (1975).
46. A. T. Amos, P. A. Brook, and S. A. Moir, *J. Phys. Chem.*, **92**, 733 (1988).
47. J. C. Gay, *et al.*, *Phys. Rev. Lett.*, **38**, 561 (1977).
48. M. Bowker and R. J. Madix, *Surface Sci.*, **95**, 190 (1980).
49. B. A. Sexton and A. E. Hughes, *Surface Sci.*, **140**, 227 (1984).
50. W. H. Press, *et al.*, *Numerical Recipes*, Cambridge Univ. (1986).
51. I. Mayor, *Int. J. Quant. Chem.*, **29**, 73 (1986).
52. B. Weiner, C. S. Carmer, and M. Frenklach, *Phys. Rev. B*, **43**, 1678 (1991).

Appendix

The integral over a contour in the complex energy plane

is given as follows. With

$$G = G_{re} + i G_{im} \quad (18)$$

and

$$E = E_{re} + i E_{im}, \quad (19)$$

the integral becomes

$$\begin{aligned} \int_C G dE &= \int_C (G_{re} + i G_{im})(dE_{re} + i dE_{im}) \\ &= \int_C (G_{re} dE_{re} - G_{im} dE_{im}) + i \int_C (G_{re} dE_{im} + G_{im} dE_{re}) \\ &= \int_\alpha (-G_{im} dE_{im} + i G_{re} dE_{im}) + \int_\beta (G_{re} dE_{re} + i G_{im} dE_{re}) \\ &\quad + \int_\gamma (-G_{im} dE_{im} + i G_{re} dE_{im}) \end{aligned} \quad (20)$$

where the paths α , β and γ are shown in Figure 1(b). Since it has been established that^{27,45}

$$G_{re}(E_{re} - i E_{im}) = G_{re}(E_{re} + i E_{im}), \quad (21)$$

$$G_{im}(E_{re} - i E_{im}) = -G_{im}(E_{re} + i E_{im}), \quad (22)$$

only the upper half of the path is required. The charge-density bond-order matrix P is given as

$$\begin{aligned} P &= 2 \frac{1}{2\pi i} 2i \left(\int_{c1} G_{re} dE_{im} + \int_{c2} G_{re} dE_{im} + \int_{c3} G_{re} dE_{im} \right) \\ &= \frac{2}{\pi} \left(\int_{c1} G_{re} dE_{im} + \int_{c2} G_{im} dE_{re} + \int_{c3} G_{re} dE_{im} \right) \end{aligned} \quad (23)$$

where $c1$, $c2$ and $c3$ are shown in Figure 1(b).

The remaining task is to obtain in the real and imaginary Green's matrix, G_{re} and G_{im} . In the complex energy plane, Eq. (1) becomes

$$((E_{re} + i E_{im})\mathbf{1} - F) \cdot (G_{re} + i G_{im}) = \mathbf{1} \quad (24)$$

or

$$((E_{re}\mathbf{1} - F) + i E_{im}\mathbf{1}) \cdot (G_{re} + i G_{im}) = \mathbf{1} + i \mathbf{0}. \quad (25)$$

If the matrices are Hermitian, the $n \times n$ complex equation

$$(A + i B) \cdot (C + i D) = E + i F \quad (26)$$

is equivalent to the $2n \times 2n$ real problem⁵⁰

$$\begin{bmatrix} A & -B \\ B & A \end{bmatrix} \cdot \begin{bmatrix} C \\ D \end{bmatrix} = \begin{bmatrix} E \\ F \end{bmatrix}. \quad (27)$$

Thus Eq. (25) in a complex energy plane can be reduced to a real equation:

$$\begin{bmatrix} E_{re}\mathbf{1} - F & -E_{im}\mathbf{1} \\ E_{im}\mathbf{1} & E_{re}\mathbf{1} - F \end{bmatrix} \cdot \begin{bmatrix} G_{re} \\ G_{im} \end{bmatrix} = \begin{bmatrix} \mathbf{1} \\ \mathbf{0} \end{bmatrix}. \quad (28)$$

The Green's matrix is given as

$$\begin{bmatrix} G_{re} \\ G_{im} \end{bmatrix} = \begin{bmatrix} E_{re}\mathbf{1} - F & -E_{im}\mathbf{1} \\ E_{im}\mathbf{1} & E_{re}\mathbf{1} - F \end{bmatrix}^{-1} \cdot \begin{bmatrix} \mathbf{1} \\ \mathbf{0} \end{bmatrix}. \quad (29)$$